

5.17 ± 0.06. Selected spectral parameters are given in Table I.

The reversible processes occurring in the spectrophotometric titrations were formulated in terms of the stepwise deprotonation of the aqua ligand to give the corresponding hydroxo complexes. Accordingly, III gives $[\text{Os}_2\text{N}(\text{NH}_3)_8(\text{OH})_2]^{3+}$ at pH = 7, and IV gives $[\text{Os}_2\text{N}(\text{NH}_3)_7(\text{OH})_3]^{2+}$ at pH = 9. That the ammine protons probably remain intact is supported by the independence of the spectra of I and II over the pH range 1-9. Alternate formulations for the deprotonated complexes in terms of oxo ligands are unlikely since higher Os oxidation states are required to stabilize the coexistence of powerful electron-donating nitrido and terminal oxo ligands.^{2-10,18-22} In comparison with Os(III) aqua complexes, the existence of the high formal oxidation state of the metal in III and IV does not lead to particularly acidic aqua ligands.²⁰⁻²³ Thus, like the oxo ligand,²¹ the nitrido ligand moderates the otherwise expected intense polarization of other ligands in the coordination sphere.

Electronic Spectra. As shown in Table I, the nitrido-bridged Os(IV) compounds display an intense absorption band in the UV region, as do mononuclear halo ammine complexes of Os(III) and Os(IV). Since the assignment of halogen-to-metal LMCT attributed to the bands of the mononuclear complexes¹⁸ cannot be adopted for III and IV, an alternative assignment was sought. A molecular orbital scheme for the isoelectronic oxo-bridged $\text{Ru}_2\text{Cl}_{10}\text{O}^{4-}$ ion has been proposed²⁴ and applied to the spectra of a number of oxo-bridged complexes.^{25,26} Following these workers, we assign the intense bands in Table I as the metal-centered π^n to π^* transitions (e_g to e_u^*). The orbitals involved in the Os-N-Os π -bonding are the d_{xz} and d_{yz} orbitals on the Os atoms and the p_x and p_y orbitals on the N atom. Our assignment is consistent with the decrease in energy of the transition on changing from an aqua ligand to Cl^- or OH^- since π -donation from the latter ligands would destabilize the d_{xz} and d_{yz} orbitals.

- (20) Gilbert, J. A.; Geselowitz, D.; Meyer, T. J. *J. Am. Chem. Soc.* **1986**, *108*, 1493.
 (21) Pipes, D. W.; Meyer, T. J. *Inorg. Chem.* **1986**, *25*, 4042.
 (22) Dobson, J. C.; Takeuchi, K. J.; Pipes, D. W.; Geselowitz, D. A.; Meyer, T. J. *Inorg. Chem.* **1986**, *25*, 2357.
 (23) Gulens, J.; Page, J. A. *J. Electroanal. Chem. Interfacial Electrochem.* **1974**, *55*, 239.
 (24) Dunitz, J. D.; Orgel, L. E. *J. Chem. Soc.* **1953**, 2594.
 (25) Lever, A. B. P. *Inorganic Electronic Spectroscopy*, 2nd ed.; Elsevier: New York, 1984; pp 641-642.
 (26) Clarke, R. J. H.; Franks, M. C.; Turtle, P. C. *J. Am. Chem. Soc.* **1977**, *99*, 2473.

Electrochemistry. As shown by cyclic voltammetry in 5 N H_2SO_4 , the reversible IV,IV/IV,V 1e-oxidation couple ($\Delta E_p = 65$ mV) at 0.90 V vs NaSCE occurs for compound II, whereas irreversible oxidation at ca. 1.09 V vs NaSCE occurs for I. This contrasting behavior resembles results obtained with mononuclear osmium halo ammines, where the III/IV half-wave potentials increased as the ratio of ammine ligands to halogeno ligands was increased, with a transition to irreversible behavior occurring in the pentammine chloro case.¹⁸ A decrease in the cathodic current of the IV,IV/IV,V wave of II was observed relative to the anodic current as the acidity of the medium was decreased. Applying a method described earlier,¹⁸ we estimate that the pK_a of an ammine ligand on the 1e-oxidation product of II has the approximate value -1. This result represents a decrease in the pK_a of the ammine ligands of at least 10 units upon 1e oxidation of the metal, paralleling changes in ammine acidity on oxidation of the mononuclear Os(III) ammine complexes.¹⁸

DNA Staining. As described earlier,¹⁶ electron-microscopy tests showed that unpurified reaction products containing I and II plus unidentified components stained DNA with high contrast. Similar results were reported in the patent literature for a material obtained by an almost identical procedure except that anion metathesis was used to give the product as a nitrate salt.¹¹ Pure samples of I and II, however, showed little staining ability, as did the corresponding aqua complexes. Cation-exchange chromatography fractions containing primarily I also produced no significant staining. Thus, the active component of the DNA stain remains as yet unidentified. Although no useful DNA-staining behavior was found with complexes I-IV, the highly contrasting, specific DNA staining possible with unpurified mixtures represents strong motivation to continue to characterize this chemistry.

Acknowledgment. This research was sponsored by the U.S. Department of Energy under Contract No. DE-AC05-84OR21400 with Martin Marietta Energy Systems, Inc., through the Exploratory Studies Program ("Seed Money") at Oak Ridge National Laboratory. This research was also supported in part by NSF Grant No. 8501261 (A.L.O.). We thank Dr. Donald E. Olins for suggestions made at the beginning of this project.

Supplementary Material Available: Figure 2, showing the UV absorbance changes of IV in the pH range 1-9, Figure 3, showing the absorbance data fitting for III, Table II, containing IR data for I and II, and a description of the SAS code containing experimental data and equations for pK_a calculations together with selected output (17 pages). Ordering information is given on any current masthead page.

Contribution from the Department of Chemistry, University of Florence, Via Gino Capponi 7, 50121 Florence, Italy, and Institute of Agricultural Chemistry, University of Bologna, Viale Bertini Pichat 10, 40127 Bologna, Italy

¹H NOE Studies on Dicopper(II) Dicobalt(II) Superoxide Dismutase

Lucia Banci,[†] Ivano Bertini,^{*†} Claudio Luchinat,[‡] Mario Piccioli,[†] Andrea Scozzafava,[†] and Paola Turano[†]

Received December 28, 1988

Substitution of zinc(II) with cobalt(II) in copper zinc superoxide dismutase gives rise to a derivative suitable for ¹H NMR investigation owing to the magnetic coupling between the two metal ions. ¹H NOE measurements have been performed in order to relate them to interproton distances. Success has been obtained with pairs of protons less than 3.5 Å apart one from the other in the copper domain. The three signals for each histidine have been assigned on a firm basis and the implications for the interaction of anions with copper discussed.

Introduction

Bovine superoxide dismutase (SOD hereafter) is a dimeric enzyme, MW 32000, whose active site contains an heterodinuclear copper-zinc chromophore.^{1,2} The X-ray structure, solved at 2.0-Å

resolution, has shown that the copper ion is bound in a distorted five-coordinate geometry to a water molecule and to four histidines, one of them acting as a bridging ligand to the proximal zinc atom.³

- (1) (a) Fridovich, I. *Annu. Rev. Pharmacol. Toxicol.* **1983**, *23*, 239-257.
 (b) Fridovich, I. *Adv. Enzymol. Relat. Areas Mol. Biol.* **1987**, *58*, 61-97.
 (2) Fee, J. A. In *Oxygen and Oxy-Radicals in Chemistry and Biology*; Rodgers, M. A. J., Power, E. L., Eds.; Academic Press: New York, 1981.

[†] University of Florence.
[‡] University of Bologna.

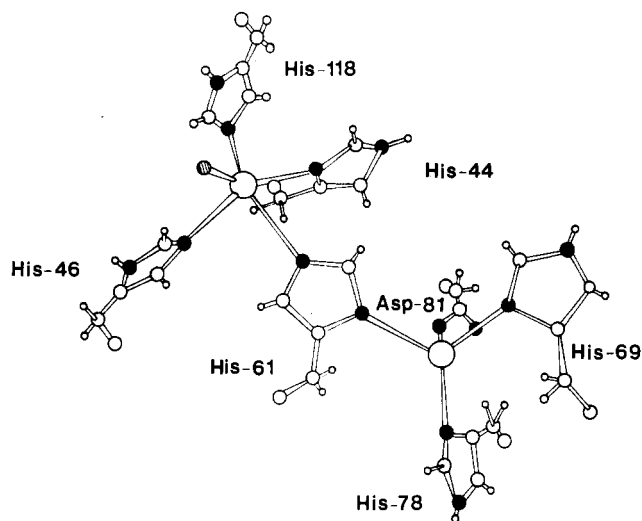


Figure 1. Schematic drawing of the copper-cobalt active site in bovine superoxide dismutase.

Two other histidines and an aspartate residue are coordinated to the zinc ion in a pseudotetrahedral geometry (Figure 1). The copper(II) and zinc(II) ions can be substituted by other divalent ions like cobalt(II), copper(II), nickel(II), etc., but activity is retained only by those derivatives that maintain copper(II) into the native site.^{4,5}

$\text{Cu}_2\text{Co}_2\text{SOD}$ is a derivative in which the native zinc ion is substituted with cobalt(II).⁶⁻¹⁰ Its catalytic properties are virtually the same as those of the native protein. As in the native copper-zinc pair, the copper and cobalt ions are linked through a histidinato bridge; the presence of such a bridge provides anti-ferromagnetic coupling between the $S = 1/2$ and $S = 3/2$ spin states.¹¹ The cobalt(II)-substituted enzyme is quite suitable for ^1H NMR investigation since the copper(II) ion in this derivative turns out to have quite short electronic relaxation times, as a consequence of the magnetic coupling with the fast-relaxing high-spin cobalt(II) ion.^{12,13} The ^1H NMR spectra of ligand nuclei in paramagnetic compounds can be easily observed when the electronic relaxation times of the paramagnetic centers are short.^{14,15}

The ^1H NMR spectrum of $\text{Cu}_2\text{Co}_2\text{SOD}$ shows as many as 19 signals that are shifted from their diamagnetic ($\text{Cu}_2\text{Zn}^{112}$ derivative) positions. Their detailed assignment is important in order to monitor the interaction of the enzyme with inhibitors and substrates. Two major studies from this laboratory dealt with the assignment of the ^1H NMR spectra and with the electronic structure of this system.^{12,13} The assignment of these signals was performed through the following three criteria:¹³ (i) the ex-

changeability of histidine NH signals and therefore their disappearance when the spectra are recorded in D_2O ; (ii) the shift position in presence of N_3^- ; (iii) the T_1 and T_2 values. The first criterion allowed us to unambiguously assign the NH protons of the five histidines coordinated to the metal ions, the bridging one having of course no such protons. The second criterion is based on the fact that anions bind selectively to the copper ion, thereby conceivably altering the isotropic shifts of the protons of copper ligands much more than those of the protons of the cobalt ligands. This criterion allowed us to discriminate between the two sets of protons. The third criterion is based on the dipolar part of the hyperfine coupling between the unpaired electrons of each metal ion and the resonating protons. The T_1^{-1} values are essentially proportional to the square of the dipolar coupling energy, and therefore they depend on the inverse sixth power of the distance between unpaired electrons and nuclei. The line width, and therefore T_2^{-1} , also contains contributions arising from the dipolar interaction of the nucleus with the time-averaged (static) magnetic moment of the complex, i.e. the so-called Curie relaxation.^{16,17} The magnetization depends on the applied magnetic field, and therefore the contribution to the line width depends on the square of the magnetic field; this contribution can be factorized out through measurements at various magnetic fields. T_2^{-1} (Curie), being dipolar in origin, also depends on the inverse sixth power of the electron-nucleus distance. In principle, T_1^{-1} and T_2^{-1} (Curie) should provide the distance between the nucleus and the closer paramagnetic center; however, very large ligand-centered effects turned out to be operative for the ligands of the copper domain.¹³ These effects are also dipolar in origin, but they depend on the fraction of unpaired electron delocalized onto the ligand. Owing to the smaller electron-proton distance in such a case, even small delocalization can cause large effects, thereby simulating shorter metal-proton distances when relaxation data are interpreted as originating solely from metal-centered effects. In the previous study, the ligand-centered effects were recognized to be strong and were taken as equal for all the histidine protons.¹³ By factorizing out the estimated ligand-centered effect, one can propose a detailed assignment of each isotropically shifted signal to individual ligand protons on the grounds of the metal-proton distances estimated from the X-ray data. In principle, however, the ligand-centered effects can be quite different from one proton to another, and the distance-based assignment remained tentative.

In recent years, developments in instrumental performance have made ^1H NOE experiments in paramagnetic systems possible. Such experiments were pioneered especially by the school of La Mar.¹⁸⁻²¹ These studies provide information on the proton-proton distances and therefore are a powerful tool for the assignment of NMR spectra and for obtaining structural information. We report here the results of such investigation on $\text{Cu}_2\text{Co}_2\text{SOD}$. Together with recent NMR data on a selectively deuterated $\text{Cu}_2\text{Co}_2\text{SOD}$ sample,²² data from the present experiments allow us to reassign some of the proton signals and reconfirm the assignment of others. The resulting picture sheds a new light on the binding mode of anions and possibly on the mechanism of SOD, as well as on the general issue of the electron-delocalization mechanisms on histidine imidazole rings.

Experimental Section

Native bovine $\text{Cu}_2\text{Zn}_2\text{SOD}$ was purchased from Diagnostic Data Inc., Mountain View, CA; the enzyme was used without further purification.

- (3) Tainer, J. A.; Getzoff, E. D.; Beem, K. M.; Richardson, J. S.; Richardson, D. C. *J. Mol. Biol.* **1982**, *160*, 181-217.
- (4) Valentine, J. S.; Pantoliano, M. W. In *Copper Proteins*; Spiro, T. G., Ed.; Wiley: New York, 1981; Vol. 3, Chapter 8.
- (5) Li-June Ming; Valentine, J. S. *J. Am. Chem. Soc.* **1987**, *109*, 4426-4428.
- (6) Fee, J. A.; Gaber, B. P. *J. Biol. Chem.* **1972**, *247*, 60-65.
- (7) Fee, J. A. *J. Biol. Chem.* **1973**, *248*, 4229-4234.
- (8) Beem, K. M.; Rich, W. E.; Rajagopalan, K. V.; *J. Biol. Chem.* **1974**, *249*, 7298-7305.
- (9) Calabrese, L.; Rotilio, G.; Mondovi, B. *Biochim. Biophys. Acta* **1972**, *263*, 827-829.
- (10) Rotilio, G.; Calabrese, L. In *Superoxide and Superoxide Dismutases*; Michelson, A. M., McCord, J. M., Fridovich, I., Eds.; Academic: London, 1977; pp 193-198.
- (11) Morgenstern-Baradau, I.; Cocco, D.; Desideri, A.; Rotilio, G.; Jordanov, J.; Dupre, N. *J. Am. Chem. Soc.* **1986**, *108*, 300-302.
- (12) Bertini, I.; Lanini, G.; Luchinat, C.; Messori, L.; Monnanni, R.; Scozzafava, A. *J. Am. Chem. Soc.* **1985**, *107*, 4391-4396.
- (13) Banci, L.; Bertini, I.; Luchinat, C.; Scozzafava, A. *J. Am. Chem. Soc.* **1987**, *109*, 2328-2334.
- (14) Bertini, I.; Luchinat, C. *NMR of Paramagnetic Molecules in Biological Systems*; Benjamin/Cummings: Menlo Park, CA, 1986.
- (15) La Mar, G. N.; Horrocks, W. d., Jr.; Holm, R. H., Eds. *NMR of Paramagnetic Molecules*; Academic: New York, 1973.

- (16) Gueron, M. *J. Magn. Reson.* **1975**, *19*, 58-63.
- (17) Vega, A. J.; Fiat, D. *Mol. Phys.* **1976**, *31*, 347-355.
- (18) Thanabal, V.; de Ropp, J. S.; La Mar, G. N.; *J. Am. Chem. Soc.* **1986**, *108*, 4244-4245.
- (19) Ramaprasad, S.; Johnson, R. D.; La Mar, G. N. *J. Am. Chem. Soc.* **1984**, *106*, 3632-3635.
- (20) Unger, S. W.; LeComte, J. T. J.; La Mar, G. N. *J. Magn. Reson.* **1985**, *64*, 521-526.
- (21) Thanabal, V.; de Ropp, J. S.; La Mar, G. N. *J. Am. Chem. Soc.* **1987**, *109*, 265-272.
- (22) Banci, L.; Bertini, I.; Luchinat, C.; Viezzoli, M. S. A comment on the ^1H NMR spectra of cobalt(II)-substituted superoxide dismutases with histidines deuterated in position $\epsilon 1$. *Inorg. Chem.*, in press.

Table I. NOE^a Calculated as a Function of T_1 and Interproton Distances Values from Equations 2 and 3 and $\tau_c = 1.4 \times 10^{-8}$ s

r , Å	NOE for T_1 (ms) of													
	0.5	0.75	1.0	1.5	2.0	3.0	4.0	6.0	8.0	12.0	16.0	24.0	32.0	48.0
1.6	2.3	3.4	4.5	6.6	8.6	12.4	15.9	22.1	27.4	36.2	43.1	53.2	60.2	69.4
1.7	1.6	2.4	3.2	4.7	6.2	9.0	11.6	16.5	20.8	28.3	34.5	44.1	51.3	61.2
1.8	1.2	1.7	2.3	3.4	4.4	6.5	8.5	12.3	15.7	21.9	27.2	35.9	42.7	52.8
2.0	0.6	0.9	1.2	1.8	2.4	3.6	4.7	6.9	9.0	13.0	16.6	22.9	28.4	37.3
2.2	0.3	0.5	0.7	1.0	1.4	2.1	2.7	4.0	5.3	7.8	10.1	14.4	18.3	25.2
2.4	0.2	0.3	0.4	0.6	0.8	1.2	1.6	2.4	3.2	4.7	6.2	9.1	11.7	16.6
2.6	0.1	0.2	0.3	0.4	0.5	0.8	1.0	1.5	2.0	3.0	3.9	5.8	7.6	11.0
2.8	<0.1	0.1	0.2	0.2	0.3	0.5	0.6	1.0	1.3	1.9	2.6	3.8	5.0	7.3
3.0	<0.1	<0.1	0.1	0.2	0.2	0.3	0.4	0.6	0.9	1.3	1.7	2.5	3.4	5.0
3.2	<0.1	<0.1	<0.1	0.1	0.1	0.2	0.3	0.4	0.6	0.9	1.2	1.7	2.3	3.4
3.4	<0.1	<0.1	<0.1	<0.1	0.1	0.2	0.2	0.3	0.4	0.6	0.8	1.2	1.6	2.4
3.6	<0.1	<0.1	<0.1	<0.1	<0.1	0.1	0.1	0.2	0.3	0.4	0.6	0.9	1.2	1.7
3.8	<0.1	<0.1	<0.1	<0.1	<0.1	<0.1	0.1	0.2	0.3	0.4	0.6	0.9	1.2	1.7
4.0	<0.1	<0.1	<0.1	<0.1	<0.1	<0.1	<0.1	0.1	0.2	0.3	0.4	0.6	0.8	1.2

^aThe NOE's value are reported as percentages and the minus sign is omitted.

The $\text{Cu}_2\text{Co}_2\text{SOD}$ derivative was prepared by using the previously reported methodology.^{7,23} $\text{Cu}_2\text{Co}_2\text{SOD}$ solutions were prepared in 50 mM Hepes buffer at pH 7.5 or in 10 mM phosphate buffer at the same pH adjusted by using NaOH or HCl. In order to remove the exchangeable protons, the cobalt(II)-substituted enzyme was lyophilized, dissolved in D_2O , lyophilized again, then dissolved in 1 mL of D_2O buffered with 10 mM phosphate at pH 7.5, and concentrated to 0.3 mL. The latter procedure was repeated four times at 12-h intervals, the last concentration being performed by adding 99.98% D_2O buffer. The protein concentrations in the NMR samples were as high as 10–15 mM.

¹H NOE measurements have been performed with a Bruker MSL instrument operating at 200.13 MHz, a Bruker CXP instrument operating at 300.06 MHz, or a Bruker AM instrument operating at 500 MHz. A total of 8K data points were collected over a 50-kHz bandwidth by using a superWEFT²⁴ pulse sequence ($180^\circ\text{-}\tau\text{-}90^\circ\text{-AQ} + \text{delay}$) with recycle times AQ + delay of 83 ms and τ values ranging from 69 to 78 ms, in order to suppress the solvent signal. Selective saturation of the signals was performed by using a selective decoupling pulse of 0.01–0.02 W kept on for $9/10$ ths of the τ values. Difference spectra were collected directly by applying the decoupler frequency on and off resonance alternately according to the following scheme: ω_2 ; $\omega_2 + \delta$; ω_2 ; $\omega_2 - \delta$. Here, ω_2 was the frequency of the irradiated signal and δ was the offset for the off-resonance irradiation, usually in the 100–500-Hz range depending on the line width of the irradiated signal and the proximity of other signals of interest. The phase of the receiver was alternated accordingly, so that a difference free induction decay was directly collected. With this acquisition scheme, the FID never saturated the computer memory and scaling did not occur even after more than 10^5 scans. We have found that cycling the decoupler frequency every scan in real time (i.e., without perturbing the steady-state pseudoequilibrium conditions set up by the superWEFT sequence) is most effective in minimizing even the smallest instabilities of the instrument and obtaining good difference spectra. The actual experiments were run in block-averaging mode; final difference spectra typically consisted of 20–40 blocks, 32 768 scans each.

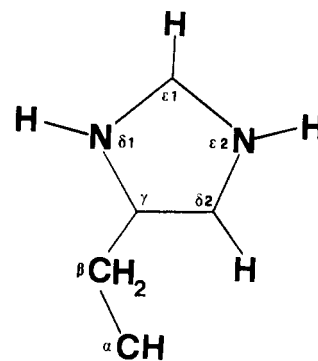
Chemical shifts were reported in ppm, calculated by assigning a 4.8 ppm chemical shift value to the solvent peak. Exponential multiplication of the free induction decay to improve the signal-to-noise ratio was such to introduce a 20–40-Hz additional line broadening.

Technical Considerations

The nuclear Overhauser effect, η_{ij} , for a proton i represents the fractional change of the intensity of signal i after saturation of the resonance of another proton, j , in the same molecular species.²⁵ η_{ij} is a function of the time t of irradiation of signal j according to

$$\eta_{ij}(t) = \frac{\sigma_{ij}(1 - e^{-\rho_i t})}{\rho_i} \quad (1)$$

where ρ_i is the intrinsic spin–lattice relaxation time of i and σ_{ij} is the cross-relaxation rate between protons i and j , which in turn,

Chart I

in the slow-motion limit operative for the present macromolecular system at 200 or 300 MHz, is given by

$$\sigma_{ij} = -\frac{\hbar^2 \gamma^4 \tau_c}{10 r_{ij}^6} \quad (2)$$

In the above expression, τ_c is the reorientation time of the vector connecting H_i and H_j , i.e. the protein tumbling time, τ_r , if local motions are not present, and r_{ij} is the interproton distance. For $t \gg \rho_i^{-1}$, eq 1 reduces to

$$\eta_{ij} = \frac{\sigma_{ij}}{\rho_i} \quad (3)$$

that so-called steady-state NOE, which is the maximum effect observable.

NOE experiments on paramagnetic macromolecules are made difficult by the large intrinsic longitudinal relaxation rates, ρ_i , which typically reduce the NOE's 10–100 times with respect to those for the diamagnetic analogues.²⁰ On the other hand, when measurable, the NOE on paramagnetic signals are virtually all primary, since spin diffusion is also quenched.²⁵ For this reason, the experiments can always be planned in such a way to reach a steady-state NOE. In the present SOD system, the largest ρ_i values for the observed paramagnetic signals are around 700 s^{-1} . For a τ_r value of 1.4×10^{-8} s as estimated from the Stokes–Einstein equation, assuming isotropic rotational motion for a MW 32 000 protein (see also later), and $\text{H}_i\text{-H}_j$ distances from 1.6 to 3.0 Å, η_{ij} values between 6.6% and 0.2% are expected. These estimates are reported in Table I as a reference for the discussion of the present experiments. From these values, it appears that, in order to detect NOE's from proton pairs more than 4.0 Å apart and for a T_1 of 8 ms, a signal to noise ratio for the difference spectra of better than 500:1 is required. Such a value constitutes the practical limit for the present experiments, given the sensitivity of the instrument and the protein concentration attainable. With this practical threshold of 4 Å, we can anticipate detection of NOE's among the paramagnetic signals between geminal protons

(23) Pantoliano, M. W.; Valentine, J. S.; Nafie, L. A. *J. Am. Chem. Soc.* **1982**, *104*, 6310–6317.

(24) Inubushi, T.; Becker, E. D. *J. Magn. Reson.* **1983**, *51*, 128–133.

(25) Kalk, A.; Berendsen, J. J. C. *J. Magn. Reson.* **1976**, *24*, 343–366.

Table II. 200-MHz ¹H NMR Shift and T₁ Values at 300 K for the Isotopically Shifted Signals in the Cu₂Co₂SOD Derivative together with Their Assignment

signal	δ, ppm	T ₁ , ^a ms	assignment
A	66.2	1.5	His-61 Hδ2 ^b
B	56.5	7.8	His-118 Hδ1 ^b
C	50.3	4.2	His-44 Hε2 ^b
D	49.4	3.8	His-69 Hδ2 ^{b,c}
E	48.8	4.6	His-78 Hδ2 ^{b,c}
F	46.7	2.1	His-78 Hε2 (His-69 Hε2) ^c
G	40.6	3.5	His-44 Hδ2 ^b
H	39.0	1.8	His-118 Hε1 ^b
I	37.4	1.7	Asp-81 Hβ1 (Asp-81 Hβ2) ^c
J'	35.6	1.7	Asp-81 Hβ2 (Asp-81 Hβ1) ^c
J	35.4	d	His-69 Hε2 (His-78 Hε2) ^c
K	34.5	8.0	His-46 Hδ1 ^b
L	28.4	4.3	His-46 Hδ2 ^b
M	25.3	2.7	His-44 Hε1 ^b
N	24.1	2.9	His-118 Hδ2 ^b
O	19.6	1.9	His-46 Hε1 ^b
P	18.7	1.6	His-44 Hβ1 ^b
Q(R)	-6.2	2.4	His-69 Hβ2 ^b
R(Q)	-6.2	2.4	His-44 Hβ2 ^b

^a Estimated error within ±15%. ^b Consistent with NOE measurements, present work. ^c References 13 and 22. ^d Not measured because the signal is within a complex envelope.

Table III. Line Width (Hz) at 300 K for the ¹H NMR Signals of Cu₂Co₂SOD at Various Magnetic Fields^a

signal	line width at				
	60 MHz	90 MHz	200 MHz	300 MHz	400 MHz
A	230	220	360	440	512
B	115	110	130	115	124
C	150	120	170	230	310
D	180	170	200	295	395
E	120	170	195	295	395
F	200	190	270	460	540
G	130	130	160	240	284
H	220	260	240	320	360
I	380	290	395	520	630
J'	480	280	410	550	930
J	280	160	275	350	474
K	160	80	80	95	117
L	190	106	160	200	255
M	160	115	210	240	280
N	160	120	205	235	280
O	250	190	250	280	340
P	330	250	340	480	530

^a Taken from ref 13.

in histidine or aspartate β-CH₂'s (r_{ij} ≈ 1.6–1.7 Å), as well as between protons adjacent one to the other on histidine rings (r_{ij} ≈ 2.4–2.5 Å), such as the nitrogen-bound Hε2 with Hε1 and Hδ2, or the nitrogen-bound Hδ1 with Hε1 (Chart I). These NOE's alone would give precious information on the assignment of groups of protons to the same residue. Furthermore, a few interproton distances among different residues may be short enough to yield NOE's, thereby helping in establishing spatial relationships among different residues. Finally, some protons may give NOE's on the other protons belonging to noncoordinated residues that, albeit at a longer distance, may still be detectable because of the smaller paramagnetic effects and hence the longer T₁'s.

Results

¹H NOE Experiments in H₂O. The ¹H NMR spectrum of Cu₂Co₂SOD in H₂O at pH 7.5 recorded at 200 MHz and 300 K is reported in Figure 2a. As previously reported,^{12,13} we observe five exchangeable protons, which are labeled as B, C, F, J, and K. The analysis of T₁ (Table II) and line width as well as of the dependence of the latter on the magnetic field of such signals (Table III), together with the larger isotropic shift changes upon addition of anions, induced us to assign B, C, and K to the NH protons of the histidines of the copper domain.¹³ We note that



Figure 2. ¹H NMR spectra of Cu₂Co₂SOD in H₂O at 300 K: (a) reference spectrum at 200 MHz; (b–g) steady-state NOE difference spectra obtained by saturating peaks B (b), C (c), K (d), G (e), M (f), and A (g), respectively. All of the spectra were recorded at 200 MHz except spectrum b, which was recorded at 300 MHz. The lower trace for each difference spectrum shows the observed signals that undergo the NOE with the vertical expansion displayed in the figure.

Table IV. Observed Nuclear Overhauser Enhancements^a between Isotropically Shifted Signals in Cu₂Co₂SOD

saturated peaks	obsd peaks										
	A	C	D	G	H	K	L	M	O	P	Q, R
A						0.8 ^d	1.1 ^b		0.4 ^c		0.2 ^d
B					1.3 ^c						
C				1.8 ^c				1.2 ^b			
G		2.2 ^c							0.8 ^c		
K										1.7 ^c	0.7 ^d
L	0.4 ^d										
M		2.8 ^c									
P								7.0 ^c			11 ^c
Q, R			1.8 ^c	0.8 ^d			2.9 ^b			7.0 ^b	

^aThe data were recorded at 200 MHz and 300 K and are reported as percent decrease in signal intensity. The minus sign is omitted. They were obtained by simulation of the difference spectra. ^bEstimated error is $\pm 10\%$. ^cEstimated error is $\pm 20\%$. ^dEstimated error is $\pm 30\%$.

His-44 is the only histidine in the copper domain coordinated through the N δ 1 (Figure 1). Thus, the NH proton of His-44 has two vicinal protons, while the NH protons of His-46 and His-118 only have one. His-61 is bound through N ϵ 2 and N δ 1 to copper and cobalt, respectively, and hence has no exchangeable protons. Therefore, a search for signals experiencing NOE's from the above exchangeable protons should permit unambiguous identification of His-44.

The difference spectra obtained upon saturation of the exchangeable protons of the copper domain (B, C, and K) are reported in Figure 2b–d. Saturation of C induces NOE's to peaks G and M, while saturation of peaks B and K gives rise to NOE only to peaks H and O, respectively. The C signal is in a crowded region of the NMR spectrum; therefore, when C is irradiated, some saturation is also induced on the closest signals. The C–G and C–M correlations were therefore checked and confirmed by saturating signals G and M separately. Both experiments gave a NOE on signal C. The difference spectra relative to these experiments are reported in traces e and f of Figure 2; all the NOE values are reported in Table IV as a percentage of the irradiated peak intensity.

On the basis of eq 2 and 3, it is possible to calculate interproton distances. By taking from X-ray data an average value of the molecular radius of 25 Å and inserting it in the Stokes–Einstein equation, we obtain $\tau_r = 1.4 \times 10^{-8}$ s. By considering this value as the approximate reorientation time (see however later) for the C–G, C–M, B–H, and K–O pairs of protons, we calculate interproton distances of 2.4, 2.4, 2.3, and 2.5 ± 0.3 Å, respectively, all consistent with the hypothesis of vicinal protons in histidine rings. This experiment leads to a new assignment of the exchangeable protons of the copper domain. The fact that C is connected through a NOE to two other ring protons unambiguously assigns C as H–N δ 2 of His-44 and G and M as the other two CH ring protons of His-44. The NOE from B to H and from K to O reveals that the pairs of protons K–O and B–H arise from two different histidines, i.e. His-46 and His-118.

The above experiments do not permit discrimination of the pairs of protons belonging to His-46 from those belonging to His-118. These two histidines have, however, different spatial relationships with respect to His-44, which is now identified, and His-61, for which a signal (Signal A) has been also identified with reasonable confidence.¹³ If, to simplify the picture, we view the four copper-coordinated histidines as lying on a square plane, then His-46 is cis to His-61 and trans to His-44, whereas His-118 is cis to His-44 and trans to His-61 (Figure 1). Of course, we may expect to observe NOE's between protons belonging to cis histidine rings but not between protons belonging to trans histidine rings. From the X-ray data, two possible inter-ring connections may be expected to be observable: (i) the H δ 2 proton of His-61, identified as signal A,¹³ may give NOE's to some of the protons of His-46; (ii) the H ϵ 1 proton of His-44 (either signal G or M) may give a NOE to the H δ 2 proton of His-118. Saturation of signal A does give rise to a NOE on signals K and L. The difference spectrum relative to this experiment is reported in trace g of Figure 2. The calculated distances, using a τ_r value of 1.4×10^{-8} s, of 3.5 ± 0.5 Å to K and 2.8 ± 0.3 Å to L, respectively, agree with K being H–N δ 1 and L being H–C δ 2 of His-46 and establish K, L, and

O as the three protons of His-46. By inference, we can assign signals B and H to H δ 1 and H δ 2 of His-118, respectively.

¹H NOE Experiments in D₂O. The ¹H NMR spectrum of Cu₂Co₂SOD in D₂O at 200 MHz and 300 K is shown in Figure 3a. As previously reported, there are seven signals that can be assigned to the copper domain owing to their T_1 values and their behavior with inhibitors. NOE experiments involving all the nonexchangeable protons of the copper domain have been carried out in D₂O in order to eliminate dynamic range limitations due to the solvent peak and to improve the sensitivity of the experiments.

In the first place, the NOE experiment on signal A, which was crucial for identification of His-46 protons, was performed also in D₂O (Figure 3b). The previously observed NOE to peak L was confirmed (Table IV). In addition, smaller NOE's were detected to O and to the unresolved—and previously unassigned—upfield signals labeled Q and R. The former confirms the assignment of O as the H ϵ 1 proton of His-46. Saturation of L (trace C) gives a sizable NOE to P, and smaller NOE's to (Q)R and A. Saturation of P (trace d) gives rise to a strong NOE to L and an even stronger NOE to (Q)R. Quantitative analysis of these data leads to a distance of 2.3 ± 0.3 Å between L and P, 2.5 ± 0.3 Å between L and (Q)R, and 1.6 ± 0.2 Å between P and (Q)R. The latter is consistent with P and (Q)R being geminal protons. Complete saturation of the upfield signal, (Q)R, reported in Figure 3e, gives a NOE to P, confirming that P, and not the nearby O signal, is the one coupled to (Q)R. Weaker NOE's are detected to L, D, and G. A NOE to L confirms that one of the two (Q)R signals is, together with P, one of the geminal protons of the β -CH₂ of His-44. The same signal could be responsible for the NOE to G, whereas the NOE to D could come from the other signal. Since D is assigned to ring protons of a cobalt-coordinated histidine, the other signal in the Q and R pair should arise from a proton far enough from the P, L, and G protons not to contribute to their NOE's. Discrimination between Q and R could be achieved with NOE studies of an anion derivative of Cu₂Co₂SOD where the Q and R signals are resolved. This is however outside the aim of the present paper. What is clearly apparent from the present data is that the L–P–(Q)R system can be univocally identified with His-46 H δ 2–His-44 H β 1–His-44 H β 2.

Saturation of signals G, H, M, N, and O has been performed, and no NOE has been detected on any isotropically shifted signal. These data support the proposed assignment: as observed before, the only pair of nonexchangeable protons that could, in principle, give rise to a NOE is H ϵ 1 of His-44 and H δ 2 of His-118. From the present data, the only remaining candidate for H δ 2 of His-118 is signal N. H ϵ 1 of His-44 could be either G or M. The NOE between N and G, if G is H ϵ 1 of His-44, should be small but observable. Since it is not observed either upon irradiation of N or upon irradiation of G, M becomes the most likely candidate for H ϵ 1 of His-44. Of course, it should also give a NOE to N. However, owing to the very small difference between the chemical shifts of the M and N signals the NOE between them is likely to be masked by even small off-resonance effects. Attempts to discriminate between off-resonance and NOE effects were unsuccessful. The observation of a small NOE between (Q)R and G confirms the assignment of G as the H δ 2 of His-44.

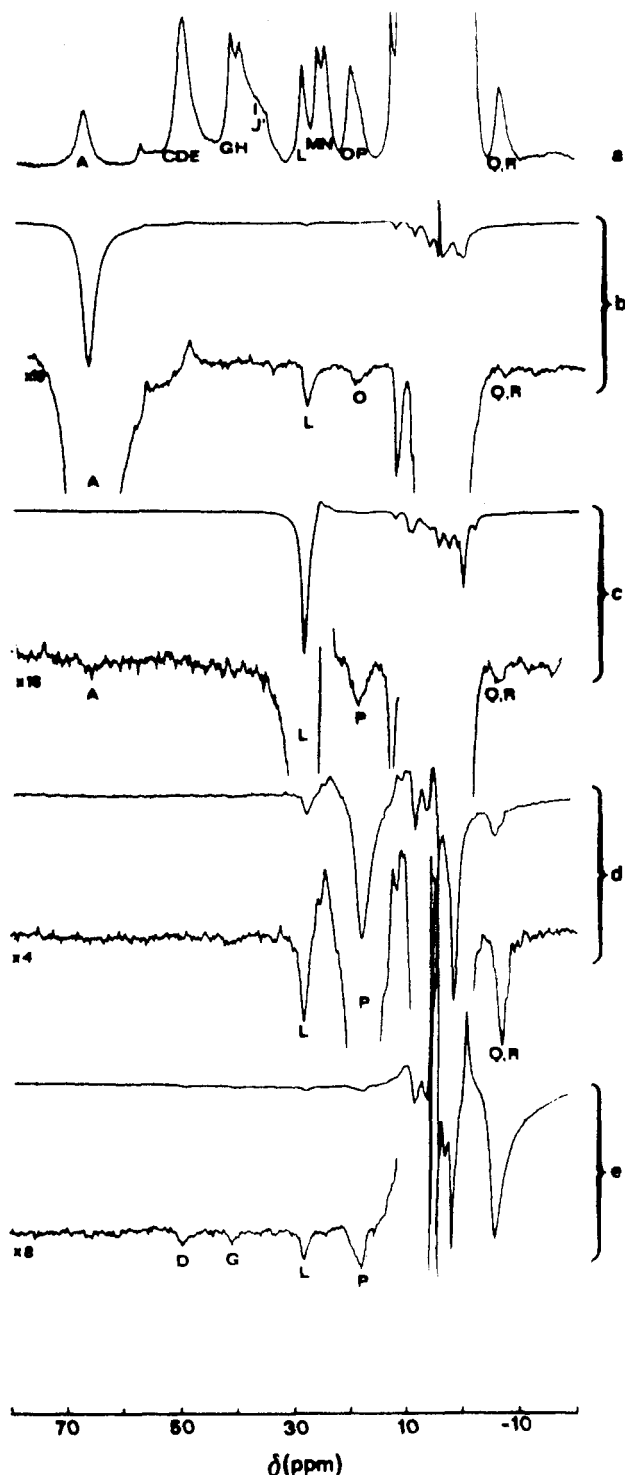


Figure 3. ^1H NMR spectra of $\text{Cu}_2\text{Co}_2\text{SOD}$ in D_2O at 300 K: (a) reference spectrum at 200 MHz; (b–e) steady-state NOE difference spectra obtained by saturating signals A (b), L (c), P (d), and Q (e), respectively. All of the spectra were recorded at 200 MHz. The lower trace for each difference spectrum shows the observed signals that undergo the NOE with the vertical expansion displayed in the figure.

It should be noted that in the difference spectra of Figures 2 and 3 several NOE's are observed in the +13 to –2 ppm region; their assignment, however, is beyond the scope of this communication.

Discussion

Reliability of the Assignment. The estimated errors in the NOE measurements range between 10 and 30% depending on the signal to noise ratios achieved and on the line width of the signals. The errors in T_1 measurements are around 10–15%. With these limitations in mind, we have recalculated τ_c values for those protons

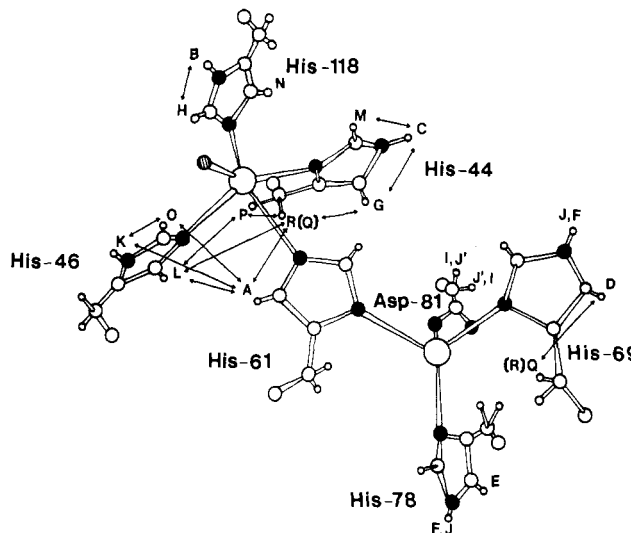


Figure 4. Active site of copper cobalt superoxide dismutase showing the correlations obtained through NOE and the assignment of the signals.

belonging to the same histidine ring or $\beta\text{-CH}_2$ groups. For these pairs, we can safely assume that the interproton distances are known to a large degree of accuracy. The τ_c values obtained are in the range $(1.3\text{--}2.4) \times 10^{-8}$ s, in good agreement with the simplistic estimate of 1.4×10^{-8} s made before. The spreading of τ_c values translates into very small discrepancies between calculated and experimental interproton distances owing to the r^{-6} dependence, therefore making the correlations established via NOE's extremely safe. In most of the cases, there is already enough discrimination in the fact that we observe or do not observe NOE's more than in quantitating the effects. As should be clear from inspection of Table I, the useful distance window covered by NOE's among paramagnetically shifted signals is extremely narrow. This makes extensive assignments based on large connectivity networks extremely difficult on one hand while allowing a very selective insight into the first and second sphere from the metal ions on the other.

The spreading of the recalculated τ_c values might at least in part be due to intrinsic rotational anisotropy of the system. Anisotropy is surely present to some extent in this dimeric protein, in which the two monomers are roughly spherical, and therefore the dimer shows a marked elongation in one direction. However, we feel that much of the present spreading is due to experimental uncertainty in the NOE values as exemplified by the NOE of C to M giving a τ_c of 1.5×10^{-8} s and of M to C giving a τ_c of 2.2×10^{-8} s. The fact that the average value of recalculated τ_c is somewhat larger than the Stokes–Einstein estimate is consistent with just a slight increase in the macroviscosity of the protein solution. It is well-known that, although the microviscosity of such a concentrated protein solution is relatively high, the effective microviscosity experienced by macromolecules is not as high as the former, until the solute volume is a sizable fraction of the total volume.

The final assignment of each isotropically shifted signal which arises from NOE connectivities is summarized in Figure 4 and Table II, fourth column. It can be noted that little information has been obtained through NOE experiments on the signals in the cobalt domain, probably because the T_1 values are too short. In a way this is consistent with the assignment of the protons of the cobalt and copper domains obtained on the basis of nuclear relaxation. The NOE measurements on the protons of the copper domain confirm which set of three signals belongs to the same histidine.

Finally, it should be noted that the assignment is consistent with the spectra obtained on $\text{Cu}_2\text{Co}_2\text{SOD}$ derivatives in which the histidines have been selectively deuterated in the $\epsilon 1$ position (Chart I).²²

Consequences of the New Assignment. From inspection of Table II, it should also be noted that signal L, which has the longest T_1 among the nonexchangeable protons of the copper domain, is

Table V. ^1H NMR Shift and T_1 Values^a and Estimated Cu-H Distances for the Protons of His-46 in $\text{Cu}_2\text{Co}_2\text{SOD}$ at 300 MHz and 303 K in the Presence of a Saturating Amount of N_3

signal	His-46 proton	shift value, ppm	T_1 , ms	$r_{\text{Cu-H}}$, Å
K	Hδ1	15.9	19.1	5.0
L	Hδ2	12.5	10.9	4.4
O	Hε1	10.5	2.8	3.4

^a Taken from ref 13.

not the farthest from the metal, but it is just an ortho-like proton of a histidine (His-46). This is the surprising result from the theoretical point of view: it means that the T_1 -distance correlation may break down even from a qualitative point of view. A possible explanation for this inconsistency is that ligand-centered effects are, at this stage of our knowledge, absolutely unpredictable and that the Hε2 of His-46 has the smallest ligand-centered contribution with respect to the other ortho-like protons. A careful inspection of the structure shows that such a proton is very close to the z axis of an xy plane formed by the coordinating nitrogens of the other histidines. If the unpaired electron is mainly delocalized into this xy plane, the metal-centered point dipole model may fail, and delocalization of the unpaired electron within the cage formed by the donor atoms might instead be considered. If this qualitative picture holds true, then signal L is the one experiencing the smallest contribution from the delocalization of the unpaired electron in the xy plane. The problem of the deviations from the point dipole model has been discussed by Golding and Golding and McGarvey with respect to pseudocontact shifts.^{26,27} In any case, in the present system the T_1^{-1} ratio between ortho-like and meta-like protons (the three histidine NH, besides

signal G) is always much smaller than the value of 15-20 expected on the basis of the r^6 dependence. Although a lengthy discussion of the general problem of unpaired electron spin delocalization on histidine rings is not appropriate here, we would like to draw attention to the experimental fact that while copper(II) in SOD seems to induce efficient delocalization into its histidine ligands, this does not hold for nickel(II) or cobalt(II) in the zinc site. For the former there is about 1 order of magnitude difference in both T_1^{-1} and line widths between ortho- and meta-like protons; for the latter, the recent experiments on the his-deuteriated sample²² have established that the ortho-like protons on the cobalt side in SOD are so broad to have always escaped detection. Clearly, this is an important issue to be addressed by everyone wishing to relate distances to T_1 values in this kind of system. In particular, unpaired spin delocalization mechanisms onto histidine rings should be better understood. Work is currently being planned to this end.

Anion Binding. The new assignment leads to the important conclusion that when cyanide and azide interact with copper, the histidine whose interaction with the paramagnetic center is virtually abolished is His-46 instead of His-44. Therefore, anions bind at a site between Arg-141 and the metal, where the semicoordinated water is located. By considering the experimental T_1 of the protons of His-46 in the azide adduct and making the reasonable assumption that ligand centered contributions have dropped to zero, it is possible to estimate new Cu-H distances through a metal-centered dipolar model, and the results are shown in Table V. It is possible that, besides small movements of His-46, the major change involves the copper ion itself, which could move up into the plane formed by the anion and the three nitrogens of the other histidines and away from His-46.

Acknowledgment. We are thankful to Prof. G. N. LaMar for guiding us in the field of NOE of paramagnetic molecules. Thanks are also expressed to Drs. J. A. Tainer and E. D. Getzoff for a helpful discussion.

(26) Golding, R. M. *Mol. Phys.* **1964**, *8*, 561.

(27) Golding, R. M.; Pascual, R. O.; McGarvey, B. R. *J. Magn. Reson.* **1982**, *46*, 30-42.

Contribution from the Laboratory for Molecular Structure and Bonding, Department of Chemistry, Texas A&M University, College Station, Texas 77843

Interactions between Cyanoborohydrides and $\text{Cl}_2\text{Pt}(\text{dppm})$. X-ray Structural Characterization of the Complexes $[\text{Pt}(\text{dppm})(\text{CNBH}_2\text{CN})]_2 \cdot \text{CHCl}_3$, $[\text{Pt}(\text{dppm})(\text{CN})]_2 \cdot \frac{1}{2}\text{C}_5\text{H}_5\text{N}$, and $[\text{Pt}(\text{dppm})(\text{CNBH}_3)]_2 \cdot \text{H}_2\text{O}$. Isomerization of *trans*- $[\text{Pt}(\text{dppm})(\text{NCBH}_2\text{CN})]_2$ to *trans*- $[\text{Pt}(\text{dppm})(\text{CNBH}_2\text{CN})]_2$

Md. Nazrul I. Khan, Christopher King, Ju-Chun Wang, Suning Wang, and John P. Fackler, Jr.*

Received April 28, 1989

A series of complexes $[\text{Pt}(\text{dppm})\text{L}]_2$ (L = NCBH_3 (1), NCBH_2CN (2), CNBH_2CN (3), CN (4), CNBH_3 (5)) have been prepared from NaBH_3CN or $\text{NaBH}_2(\text{CN})_2$ and $\text{Cl}_2\text{Pt}^{\text{II}}(\text{dppm})$ or $[\text{Pt}^{\text{I}}(\text{dppm})\text{Cl}]_2$. The particular complex or linkage isomer obtained is dependent on the choice of solvent. X-ray structural characterizations of 3-5 have been performed. The linkage isomerization of NCBH_3 upon coordination to the dinuclear platinum complex is described. With $\text{BH}_2(\text{CN})_2$, isomerization of only one BCN linkage is found in $[\text{Pt}^{\text{I}}(\text{dppm})(\text{CNBH}_2\text{CN})]_2$. Compounds 3-5 crystallize in the space groups $P\bar{1}$, $P2_1/c$, and C_2/c , respectively, with the following cell constants: $a = 12.665$ (4) Å, $b = 12.706$ (3) Å, $c = 18.297$ (5) Å, $\alpha = 75.80$ (2)°, $\beta = 82.20$ (2)°, $\gamma = 84.85$ (2)°, $V = 2833$ (3) Å³ for 3; $a = 13.773$ (7) Å, $b = 16.404$ (8) Å, $c = 21.496$ (7) Å, $\beta = 105.81$ (3)°, $V = 4673$ (4) Å³ for 4; $a = 15.719$ (2) Å, $b = 16.842$ (3) Å, $c = 20.217$ (4) Å, $\beta = 104.781$ (1)°, $V = 5176$ (1) Å³ for 5. The refinement converged to $R = 0.0414$ and $R_w = 0.0452$ for 3, $R = 0.0360$ and $R_w = 0.0365$ for 4, and $R = 0.0329$ and $R_w = 0.0524$ for 5. The Pt-Pt bond distances of 2.665 (1) Å in 3, 2.704 (1) Å in 4, and 2.667 (1) Å in 5 indicate metal-metal bonding interactions. The Pt centers in these d⁹ complexes possess square-planar geometries. The Pt-C bond distances are 1.963 (10), 1.993 (11), and 2.037 (11) Å in 3, 2.054 (9) Å in 4, and 2.015 (10) Å in 5. Complex 5 has a center of symmetry. Compounds 1 and 2 slowly isomerize in solution to 5 and 3 at room temperature and rapidly isomerize at elevated temperature via inorganic linkage mechanisms.

Introduction

Transition-metal complexes of the cyanotrihydroborate anion containing M-NCBH_3 , $\text{M-HBH}_2\text{CN}$, or $\text{M-H-BH}_2\text{-CN-M}$

linkages with a wide variety of phosphine and non-phosphine ligands have been known for several years.¹⁻¹⁰ Of particular

(1) Lippard, S. J.; Welcker, P. S. *J. Chem. Soc. D* **1970**, 515.

(2) Ford, P. C. *J. Chem. Soc. D* **1971**, 7.

(3) Vaska, L.; Miller, W. V.; Flynn, B. R. *J. Chem. Soc. D* **1971**, 1615.

* To whom correspondence should be addressed.